The Canadian Mineralogist
Vol. 39, pp. 1039-1051 (2001)

CELSIAN, (Ba,K)-FELDSPAR AND CYMRITE FROM SEDEX BARITE DEPOSITS OF ZAMORA, SPAIN

MARIA CANDELAS MORO[§], MARIA LUISA CEMBRANOS[§] and AGUSTINA FERNANDEZ[§]

Departamento de Geología, Facultad de Ciencias, Universidad de Salamanca,
Plaza de los Caídos s/n, E-37008 Salamanca, Spain

ABSTRACT

(Ba,K)-feldspars occur with cymrite as thin layers of massive fine-grained celsian interbedded with apatite, sulfides and barite, or diseminated in the thin-bedded barite-bearing siliceous and carbonate beds ranging in thickness from 0.15 to 0.40 m in three barite deposits in Zamora, Spain. The (Ba,K)-feldspars, which include celsian, hyalophane and K-feldspar, vary from 1.3 to 96.4 mole % $BaAl_2Si_2O_8$, but exhibit two discontinuities, at 8–24 and 40–92 mol.%. The associated cymrite shows 1.3–3 mol.% $KAlSi_3O_8$ in solid solution. Relict celsian has a similar K content, 1.2–2.8 mol.% $KAlSi_3O_8$. The Ba-rich feldspars may have been deposited i) as an authigenic phase, or ii) by replacement of authigenic barite during a later diagenetic or metamorphic event. Cymrite and celsian were formed under low-grade dynamothermal metamorphism that affected Paleozoic sedex barite deposits of Zamora. Fluid-inclusion studies indicate 350°–370°C and 1.5 kbars as conditions of equilibration. Those data, and the presence of vitrinite (350°C), indicate the upper limit of P–T reached. These conditions are close to the reaction curve for celsian + H_2O = cymrite. The stability field of cymrite confirms that this mineral can be stable in low-P – low-T metasedimentary environments. That reaction has geobarometric and tectonothermal importance.

Keywords: (Ba,K)-feldspars, celsian, hyalophane, cymrite, barite deposits, hydrothermal activity, low-grade metamorphism, Zamora Province, Spain.

SOMMAIRE

Des compositions de feldspath (Ba,K) se sont développées en association avec la cymrite en couches minces de celsian massif à grains fins interstratifié avec l'apatite, des sulfures, et la barite, ou bien en disséminations dans de minces horizons siliceux et carbonatés à barite allant de 0.15 à 0.40 m en épaisseur dans trois gisements de barite dans la province de Zamora, en Espagne. Les feldspaths de (Ba,K), qui comprennent celsian, hyalophane et feldspath potassique, varient de 1.3 à 96.4% de $BaAl_2Si_2O_8$ (base molaire), avec quand même deux discontinuités, à 8–24 et 40–92%. La cymrite associée contient entre 1.3 et 3% de $KAlSi_3O_8$ en solution solide. Les reliquats de celsian possèdent un teneur semblable, entre 1.2 et 2.8% de $KAlSi_3O_8$. Les feldspaths riches en Ba pourraient avoir été déposés soit comme phase authigène, soit en remplacement de la barite au cours d'un événement tardif d'origine diagénétique ou métamorphique. La cymrite et le celsian se sont formés à faible pression en milieu métamorphique affectant les gisements de barite exhalatifs paléozoïques de la région de Zamora. Les études antérieures des inclusions fluides indiquent des conditions d'équilibrage de 350°–370°C et 1.5 kbars. Ces données, ainsi que la présence de la vitrinite (350°C), témoignent des limites atteintes en termes de P et de T. Ces conditions se rapprochent des coordonnées de la réaction celsian + H_2O = cymrite. La cymrite peut avoir un champ de stabilité dans des milieux métasédimentaires à faibles pressions et températures. Cette réaction aurait une importance géobarométrique et tectonothermale.

(Traduit par la Rédaction)

Mots-clés: feldspaths de (Ba,K), celsian, hyalophane, cymrite, gisements de barite, activité hydrothermale, métamorphisme de faible intensité, province de Zamora, Espagne.

[§] *E-mail addresses*: cmoro@gugu.usal.es, cembranos@gugu.usal.es, aff@gugu.usal.es

INTRODUCTION

The barite deposits of Zamora, Spain, are hosted by Silurian–Devonian metasediments of the northwestern part of the Hesperian Massif (Alcañices Synform) and were exploited in the Ambiciosa, Maria Carmen and Astur mines. From these, a total of 50 to 60 million tonnes of barite were extracted both by underground and open-pit workings. Since 1975, the mines are inactive. The Ambiciosa mine is 2 km southwest of Vide de Alba, the Maria Carmen is 1 km west of San Blas, and the Astur mine is 2 km northeast of Nuez de Aliste (Fig. 1).

The (Ba,K)-feldspars studied were detected in thin layers interbedded with apatite, sulfides and barite or diseminated in the thin-bedded barite-bearing siliceous and carbonate beds that range in thickness from 0.15 to 0.40 m in the mineralized zone of the sedex-type barite deposits of Zamora. These deposits were studied by Poole *et al.* (1990), Hernández *et al.* (1991), and Moro *et al.* (1993, 1994).

The aim of this work is to show the mineralogical, textural and chemical characteristics of these minerals in order to establish their possible genesis, taking into account the main metallogenic characteristics of the barite deposits, and particularly their stable isotope geochemistry and results of fluid inclusion investigations. The coexistence and phase relations of celsian and cymrite are of considerable petrological interest as a natural example of the experimentally established reaction curve celsian + H_2O = cymrite (Essene 1967).

BACKGROUND INFORMATION

Celsian, hyalophane and cymrite are restricted in occurrence. They are associated typically with sedimentary and metasedimentary rocks (Bjorlykke & Griffin 1973, Reinecke 1982, Jakobsen 1990), manganese and ferromanganese deposits (McSwiggen *et al.* 1994), stratabound (syn-sedimentary) barite–sulfide deposits (Froehlich & Sandréa 1973, Coats *et al.* 1980, 1984, Chabu & Boulègue 1992, Devaraju *et al.* 1999, Fortey & Beddoe-Stephens 1982, Fortey *et al.* 1993, Hsu 1994, Kribek *et al.* 1996, Pouit & Bois 1986), and other Ba-rich rocks (Pan & Fleet 1991). Most occurrences of (Ba,K)-feldspars are associated with exhalative hydrothermal proccesses and low- and medium-grade metamorphism.

Natural occurrences of celsian, $BaAl_2Si_2O_8$, and solid solutions toward K-feldspar (hyalophane) are better documented than those of cymrite, $BaAl_2Si_2O_8 \cdot nH_2O$ (where $0 < n < 1$). Some occurrences of cymrite are associated with high-pressure, low-temperature regional metamorphism (*e.g.*, Essene 1967, Reinecke 1982, Moles 1985), whereas others were formed under near-surface sedimentary or hydrothermal conditions (*e.g.*, Runnells 1964, Froehlich & Sandréa 1973, Aye & Straus 1975, Soong & Olivecrona 1975, Coats *et al.* 1980, Fortey & Beddoe-Stephens 1982, Jakobsen 1990).

In this study, and according to Graham *et al.* (1992) the term cymrite is used for hexagonal or pseudohexagonal phases of composition $BaAl_2Si_2O_8 \cdot nH_2O$ over the compositional range $0 < n < 1$. Where $n = 0$, the phase is equivalent to "hexacelsian". The structural properties of the latter phase were discussed extensively by Viswanathan *et al.* (1992). Celsian has a monoclinic form and is stable from room temperature up to 1590°C at atmospheric pressure, where it inverts slowly and changes to "hexacelsian". The latter phase may persist metastably on cooling, but is not reported to occur naturally and is therefore thought to be unstable under crustal conditions (Lin & Foster 1968). Hyalophane occurs along the binary solid-solution series between $KAlSi_3O_8$ and $BaAl_2Si_2O_8$ (celsian). Cymrite and celsian are related by the dehydration reaction: $BaAl_2Si_2O_8 \cdot nH_2O$ (cymrite) = $BaAl_2Si_2O_8$ (celsian) + nH_2O.

GEOLOGICAL SETTING OF THE BARITE DEPOSITS

The barite deposits (Ambiciosa, Maria Carmen and Astur mines) of the Middle-Western zone of Zamora, are located in the "Central Iberian Zone" (CIZ) and in the "Galicia – Trás-os-Montes zone" (GTMZ) of the Iberian Massif (Fig. 1). They are hosted in Manzanal del Barco and Rábano formations (Alcañices Synform) characterized by Silurian to Middle Devonian metasediments. These rocks have a volcano-sedimentary origin, with varied lithologies, among which siliceous shale, black and grey chert, limestone, metavolcanic rocks, black shale, greywacke and feldspathic quartzite are the most prominent. The interstratified volcanic rocks, rhyolite, dacite and andesite, belong to the calc-alkaline series with a marked potassic trend (González Clavijo 1997).

These materials were affected by three main phases of folding of Hercynian age and a low to very low grade of regional dynamic metamorphism. The first phase (D_1) gave rise to megascopic folds and generated the regional cleavage seen in all region. The second phase (D_2) formed subhorizontal ductile shear-zones and overthrusts, and the third phase (D_3) generated open subvertical folds, mostly homoaxial with D_1 folds, and a crenulation cleavage. The regional metamorphism is characterized by a low to medium pressure and temperature of approximately 350°C, according to the measurements of the *b* parameter of muscovite and the application of the conodont index of color alteration as a geothermometer (González Clavijo 1997).

According to Moro *et al.* (1994), the similar nature of the host-rock and of morphological, textural, structural, mineralogical and geochemical characteristics of the mineralization allow a common description of the barite deposits.

1) Barite mineralization is close to very important thrust faults, which correspond to true overthrusts (González Clavijo 1997).

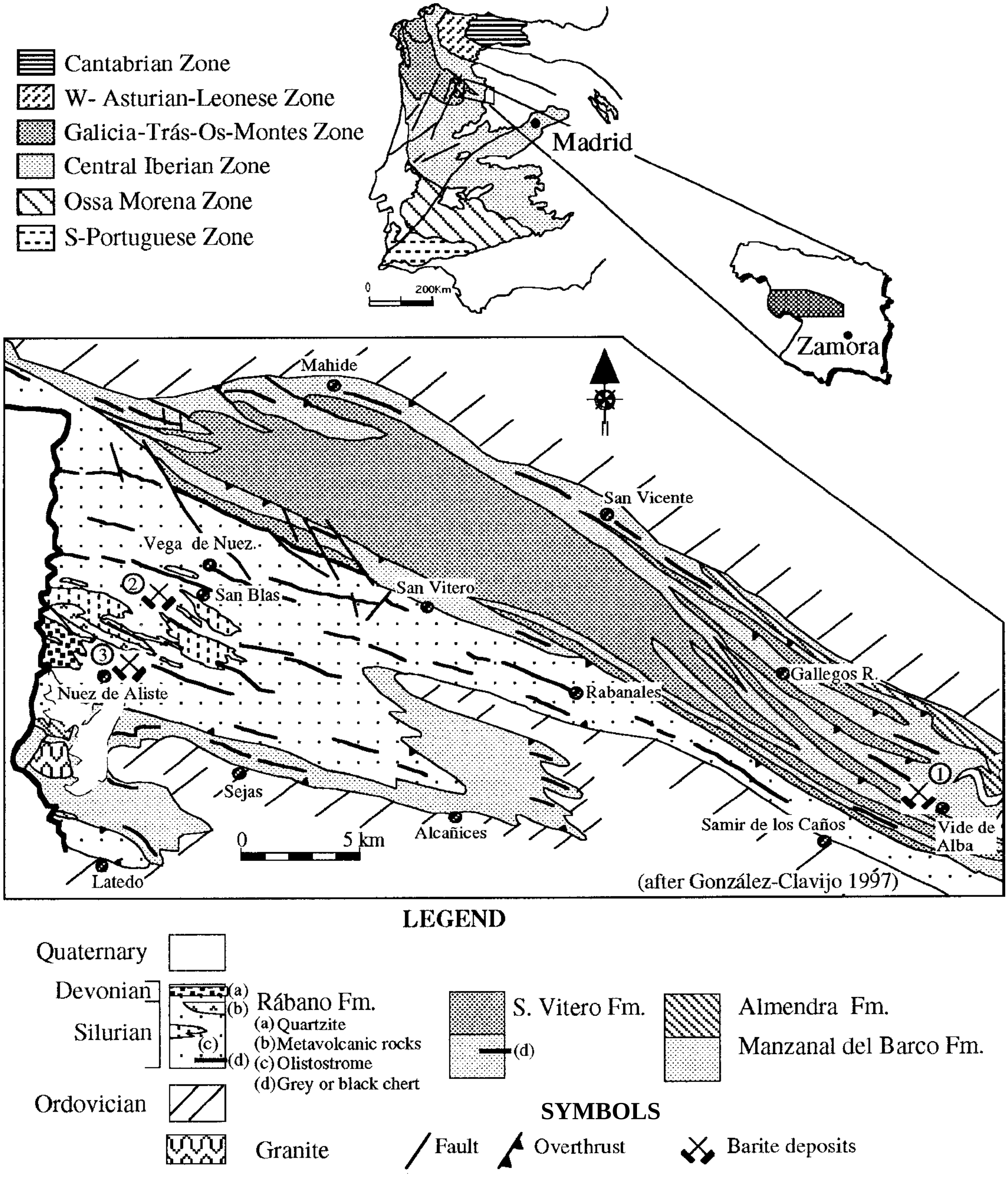

FIG. 1. Geological context of the barite deposits. In the upper part of the figure, geotectonic zones of the Iberian Massif. Below, simplified geological map of the middle to western part of Zamora Province, where the barite mines are located: (1) Ambiciosa mine, (2) Maria Carmen mine and (3) Astur mine.

2) The Astur and Maria Carmen deposits are interstratified and probably in the same stratigraphic position in the Silurian to Middle Devonian materials of the Rábano Formation (Central Iberian Zone), whereas the Ambiciosa deposit is interstratified in the Llandovery–Ludlow materials of the Manzanal del Barco Formation (Galicia – Trás-os-Montes Zone) (Fig. 1).

3) The host-rocks consist of interbedded chert, siliceous and black shale, limestone, metavolcanic rocks, greywacke and feldspathic quartzite. Chert and shale are the most important rock-types. According to geochemical data (Moro *et al.* 1994), the host rocks may well have formed in a marine continental-platform setting, the SiO_2 being provided by exhalative hydrothermal solutions channeled though deep fractures.

4) All of the barite deposits are lenticular and consist mainly of meter-thick beds of massive barite, with interbedded barite – silica – carbonate beds. At the top and bottom of these units, other thinner and more complex layers are observed. They consist of crystals, nodules, lenses and laminae of barite set in a matrix formed by quartz, white mica, barite, (Ba,K)-feldspar and carbonate. Vitrinite seams (Poole *et al.* 1990) and finely interbedded sulfides (mostly pyrite) and sulfosalts (most commonly, tetrahedrite) also are present. Both massive barite and barite-rich beds are occasionally affected by intraformational brecciation and folding, indicating a certain instability in the depositional basin.

5) Among the trace elements detected in the barite, the high content of V ($\bar{x}$ = 4825 ppm, 1σ = 38) is significant. The high content of this element suggests that the environment in which the barite deposits formed were rich in organic matter, which adsorbs V. The oxidation processes may well have released V from organic matter, later incorporated in barite.

6) The primary fluid inclusions in crystals and massive barite are two-phase assemblages, with a low-salinity (5% NaCl eq.) liquid phase and other gaseous phase constituted by very pure CO_2. According to a P–T plot, these two-phase inclusions must have been trapped between 350 and 370°C, and between 1500 and 1550 bars (Hernández *et al.* 1991).

7) From an isotopic point of view, the barite is generally enriched in ^{34}S and ^{18}O with respect to marine sulfate of the same age. This enrichment in ^{34}S detected in all samples of barite may have been imparted during the recrystallization processes, related to the diagenetic and metamorphic events. The pyrite has variable $\delta^{34}S$, which is characteristic of sedimentary pyrite formed from H_2S generated by bacterial reduction of marine sulfates. The strongly negative value of $\delta^{13}C$ of carbonates suggests that these minerals were formed from CO_2 generated by oxidation of organic matter (Moro *et al.* 1994).

8) These barite deposits could be classified as belonging to the exhalative-sedimentary type; later diagenetic and mainly metamorphic events produced the textural and structural features of the different types of barite and interbedded barite-rich rocks [barite – silica – carbonate – phosphate – (Ba,K)-feldspars and vitrinite] observed.

SAMPLES AND METHOD

The samples studied come from barite – silica – carbonate beds interlayered with beds of massive barite and the complex (foliated) layers at the top and bottom of these units (Fig. 2).

The barite – silica – carbonate beds are a major component of the mineralized zone, ranging between several cm to 40 cm in thickness. This rock has a compact, coarse granoblastic texture and contains calcite subordinate to dolomite, quartz and (Ba,K)-feldspars in addition to sulfides (mostly pyrite).

The complex (foliated) layers that range from 10 to 15 cm in thickness are dark grey and have a compact, fine-grained, granoblastic and weakly banded texture. They are generally associated with crystals, nodules, lens and laminae of barite. These rocks contain, in addition to barite, anomalous amounts of Ba-bearing feldspar and lesser quantities of quartz, white mica, organic matter, apatite and euhedral crystals of pyrite (Fig. 2). These barite-rich layers display slumping-induced microfolds and slip structures. Both types of structures have been interpreted in terms of intraformational deformation, reflecting tectonic instability in the basin where the barite deposits formed.

The Ba-feldspar-bearing samples have been studied by polarizing microscopy (P.M.) and scanning electron microscopy; we used a DSM–940 Zeiss equipment coupled to an energy-dispersion spectrometer (SEM–EDX). Electron-microprobe analyses of the Ba-rich feldspar were carried out with a Camebax SX–50 instrument. Concentrations of Si, Al, Ba, Ca, K, Na, Mg, Fe, Ti, and Mn were determined on celsian, cymrite, hyalophane and K-feldspar crystals in the samples studied. The operating conditions were: accelerating voltage 15 kV, beam current 15 nA, spot size 2 μm, and counting time 10 s. The following standards were used: orthoclase for Si and K, albite for Al and Na, andradite for Ca and Fe, celsian for Ba, $MnTiO_3$ for Ti and Mn, and MgO for Mg.

THE (BA,K)-FELDSPARS

Petrography

The microscopic observations on the (Ba,K)-feldspars in the samples studied were made with the aid of back-scattered electron imaging facilities during microprobe analysis. As seen in thin sections, the (Ba,K)-feldspars mostly occur as optically uniform crystals in which cleavage and twinning are poorly developed, except in coarse crystals, where cleavage and simple twins are not uncommon. The feldspars exhibit a distinctly lower relief compared to barite.

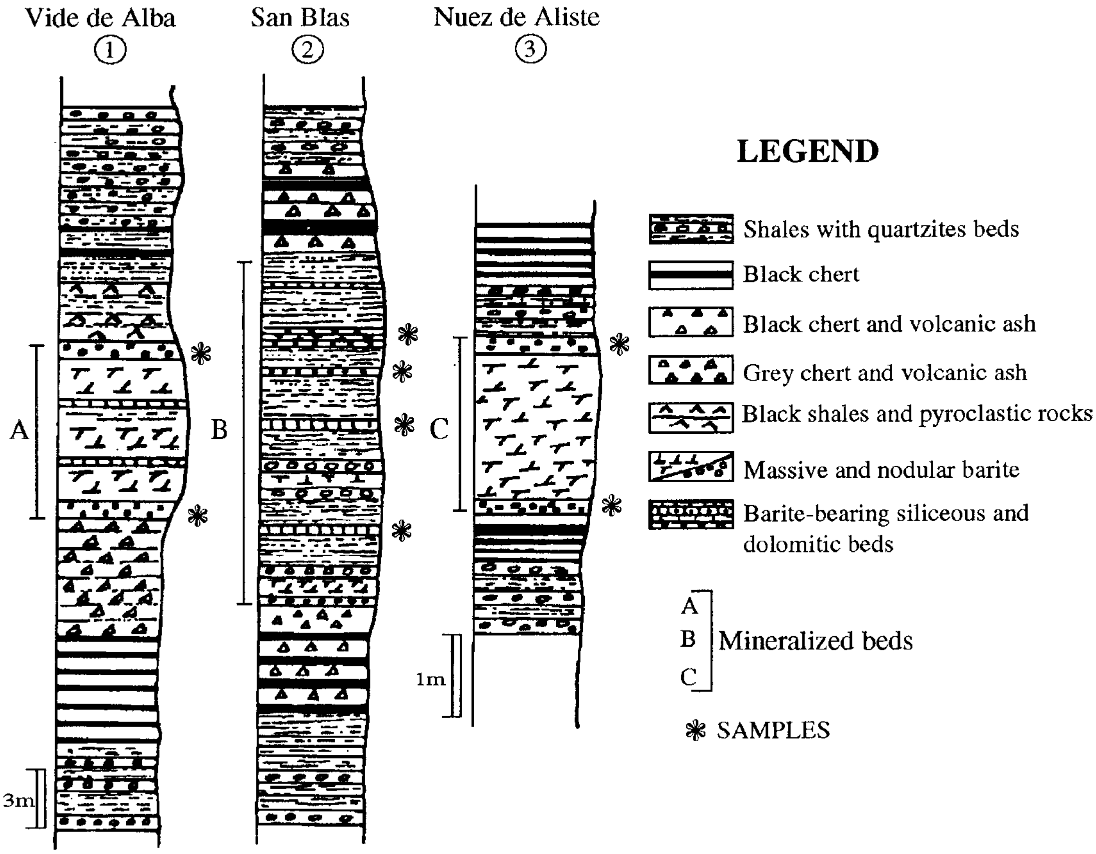

FIG. 2. Stratigraphic sections of the (1) Ambiciosa mine, (2) Maria Carmen mine and (3) Astur mine.

Celsian constitutes massive beds in which crystals range from 20 to 50 μm across; these layers are interbedded with other thin layers of fine-grained barite, microcrystalline to cryptocrystalline apatite, sulfides (mostly pyrite), and organic matter (vitrinite) (Fig. 3a). As such, they could correspond to a primary sedimentary deposit. Celsian is distinguished from cymrite by its slightly lower indices of refraction and a rare lamellar twinning (Fig. 3c). Mosaics of celsian seem to be replaced by plates of cymrite (Fig. 3d) and crystals and massive beds of barite are replaced by Ba-rich feldspar, probably during later diagenetic and mainly metamorphic processes (Figs. 3e, f, 4a, b).

Cymrite in thin section resembles celsian. It commonly occurs in fine plate-like crystals or rectangular grains about 50–100 μm in size with a pronounced cleavage parallel to (001) and a less well developed cleavage (001) (Figs. 4c, d). Cymrite is uniaxial negative, colorless, of moderate relief and low birrefringence where pure, but it is commonly dark green or brown because of inclusions and various products of alteration (Fig. 4d).

In complex (foliated) layers, the cymrite shows either a parquet-like texture in nearly monomineralic layers (Fig. 4c), or the isolated plates distributed throughout the barite-rich rocks have a poikiloblastic texture (Fig. 4d). Cymrite may have replaced a pre-existing mineral (probably celsian) in a later hydrothermal event, possibly under near-surface conditions.

Hyalophane also occurs with K-feldspar in fine crystals disseminated in barite-bearing carbonate beds (Fig. 4e). Both also occur as a thin rim and as cross-cutting veins and as filling material in tension gashes (Fig. 4f). The presence of hyalophane in these veins indicates that periods of barium mobility persisted throughout the tectonic events.

X-ray diffraction (XRD)

Attempts were made to further characterize the minerals by X-ray-diffraction methods. Owing to difficulties with separation of the fine-grained minerals, no further information on these minerals was obtained.

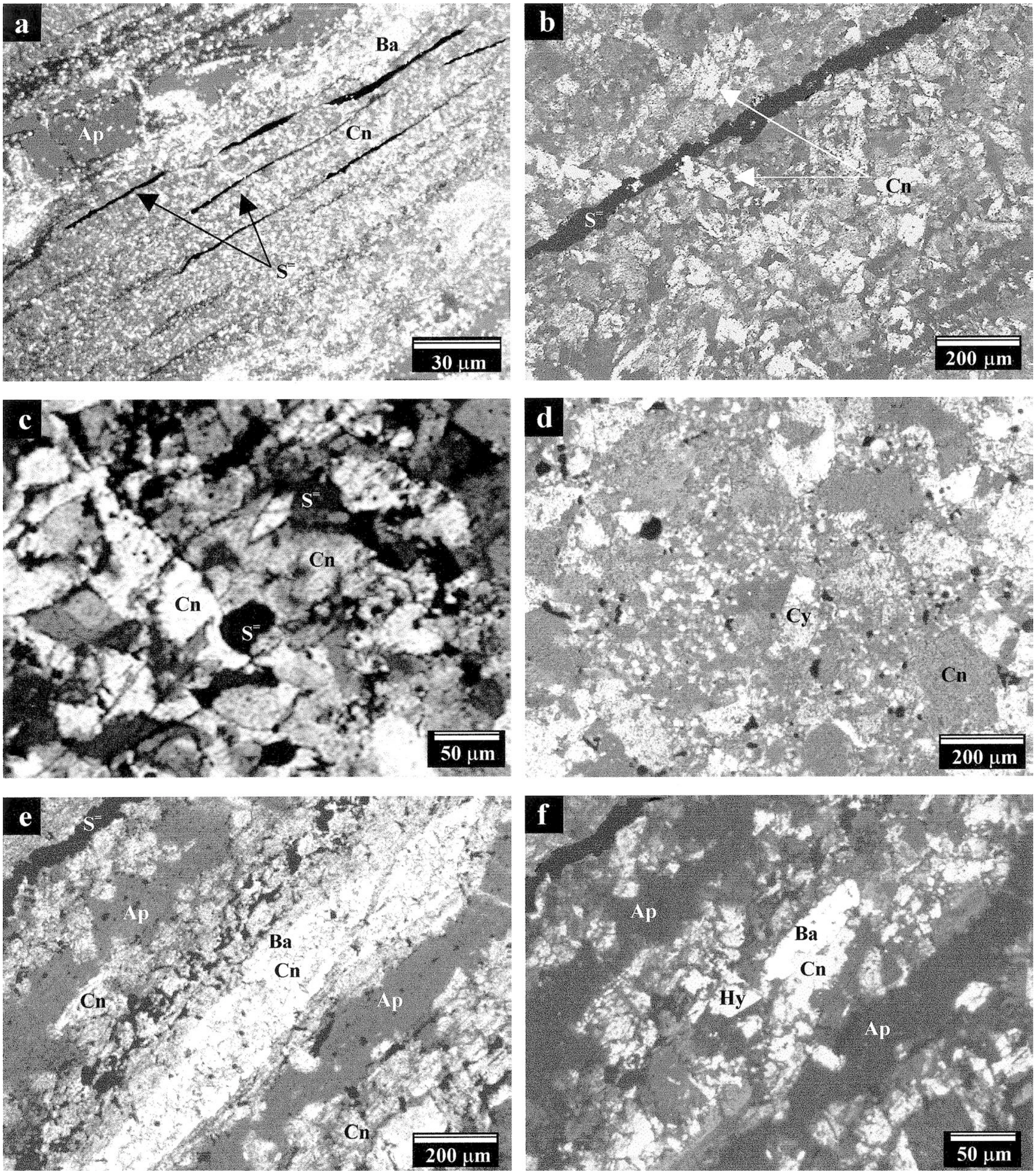

FIG. 3. (a) Parallel laminae of massive celsian (Cn), apatite (Ap), barite (Ba), sulfides ($S^=$) and organic matter (M.O.). (b) The celsian laminae are constituted by aggregates of fine crystals of celsian. (c) The coarse celsian-rich rock consists of euhedral to subhedral recrystallized crystals of celsian with disseminated anhedral crystals of pyrite. (d) The relationship between celsian and cymrite; note that the celsian crystals have been replaced by cymrite and partially by quartz. (e) The relationship among barite, sulfides and celsian. Note the overgrown, euhedral celsian (Cn) and the small anhedral crystals of pyrite set in a matrix of massive apatite and massive laminae of barite partially replaced by celsian. (f) Relict grains of barite (white) in celsian and hyalophane. Photographs taken in plane-polarized light except for (f, c), taken under crossed polars (scale in µm).

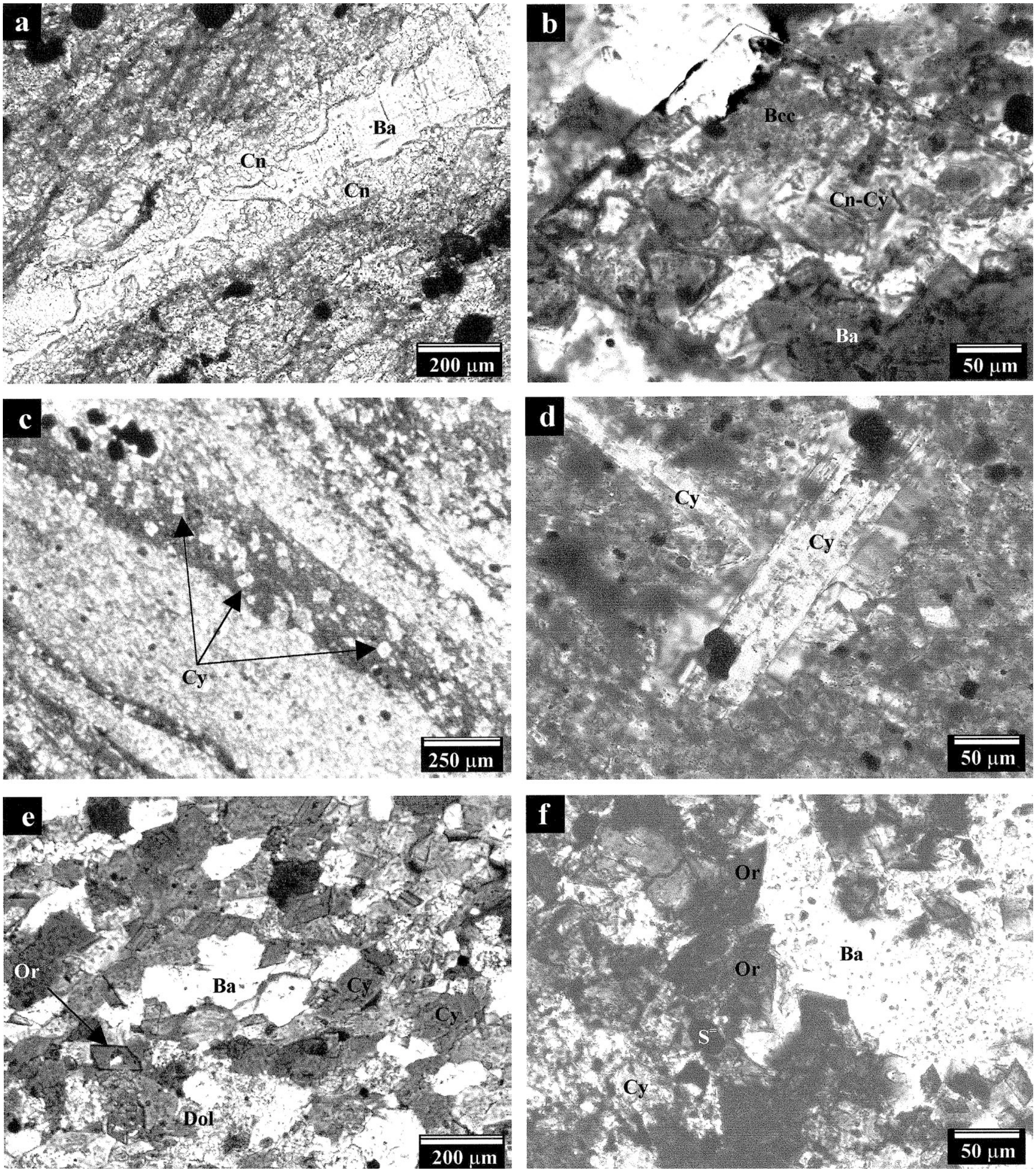

FIG. 4. (a) Detailed relationship in a barite laminae surrounded by celsian crystals. (b) Euhedral barite crystal replaced by a mixture of celsian, cymrite and barytocalcite. (c) Banded barite–muscovite schists in which disseminated cymrite crystals appear. (d) Siliceous rock containing cymrite in rectangular grains. The opaque phases are goethite and pyrite; the rest is microcrystalline quartz. (e) Barite–dolomite rock showing cymrite and euhedral crystals of K-feldspar associated with dolomite. (f) The relationship among K-feldspar, (Ba-K)-rich feldspar, cymrite and barite. The photographs taken in plane-polarized light except for (e, f), taken under crossed polars (scale in μm).

(Ba,K)-feldspars chemistry

Relatively few compositions have been reported in the literature. In this study, we provide electron-microprobe data for (Ba,K)-feldspars from Zamora province (Tables 1, 2) and from other localities (Figs. 5, 6).

In terms of a Cn–Or–Ab plot (Fig. 5), the (Ba,K)-feldspars from Zamora can be divided into four types: i) Cn-rich specimens, celsian (Table 1), with compositions $Cn_{94–96}$ $Or_{1–3}$ $Ab_{2–3}$, ii) cymrite (Table 1), with compositions $Cn_{93–97}Or_{1–3}Ab_1$, iii) specimens with an intermediate composition (Table 2): $Cn_{29–40}Or_{57–65}Ab_{4–6}$, and iv) orthoclase (Table 2), with a composition $Cn_{1–5}Or_{94–98}$. The albite content of these feldspars is minor, and does not exceed 10 mole % Ab.

The compositions obtained on celsian from these samples (Table 1) correspond closely with those previously published from Aberfeldy (Coats *et al.* 1980) (Figs. 5, 6). Most grains show an appreciable amount of Ti and Fe, which may well be due to impurities.

The chemical composition of cymrite is compatible with cymrite from Aberfeldy (Fortey & Beddoe-Stephens 1982) (Table 1, Figs. 5, 6). Assuming that the oxide deficits from 4 to 5% indicate the H_2O content (theorical value: 4.6%) (Fortey & Beddoe-Stephens 1982, Carron *et al.* 1964), the (BaO + Al_2O_3) *versus* (SiO_2 + K_2O + Na_2O) plot (Fig. 6) indicates contents from 1 to 2 moles of H_2O in the structure.

Hyalophane generally contains between 5 and 30 mole % Cn (Deer *et al.* 1992). However, hyalophane is not restricted to this compositional range, and higher contents of celsian are reported from many localities (Pan & Fleet 1991, Chabu & Boulègue 1992). The primary substitution is between BaAl and KSi (Gay & Roy 1968). The latter authors have argued that the rarity of Ba-rich feldspars is due more to the lack of suitable conditions in nature than to any fundamental difficulties in accommodating the Ba cation in the feldspar structure, and that the series $KAlSi_3O_8$–$BaAl_2Si_2O_8$ is continuous. Therefore, one should regard $BaAl_2Si_2O_8$

TABLE 1. COMPOSITION OF CELSIAN AND CYMRITE IN SEDEX DEPOSITS, ZAMORA, SPAIN

	Celsian								Cymrite									
Sample	PB-1		PB-6F		PB-6I		IF-13		SB-C		IF-11		VMSB-10		IF-2		PB-1	
Analysis	*n* = 3	σ	*n* = 4	σ	*n* = 5	σ	*n* = 2	σ	*n* = 9	σ	*n* = 3	σ	*n* = 2	σ	*n* = 3	σ	*n* = 7	σ
SiO_2 wt%	32.06	0.54	32.89	0.63	32.32	0.34	32.32	1.64	32.21	1.64	32.81	1.28	33.98	3.01	32.83	1.68	31.21	0.37
Al_2O_3	24.67	0.08	24.75	0.29	24.90	0.22	25.49	0.03	23.89	0.72	23.07	0.87	23.39	1.32	22.99	0.81	24.13	0.25
FeO(*)	0.16	0.28	0.04	0.06	0.03	0.04	0.00	0.00	0.05	0.04	0.02	0.03	0.00	0.00	0.11	0.06	0.01	0.02
CaO	0.02	0.03	0.01	0.01	0.09	0.15	0.00	0.00	0.08	0.09	0.01	0.01	0.02	0.03	0.02	0.03	0.01	0.02
BaO	41.39	0.91	41.20	0.64	42.30	0.65	40.70	2.15	38.91	1.10	37.67	0.52	37.06	2.00	38.99	0.75	39.61	0.34
Na_2O	0.18	0.11	0.24	0.07	0.16	0.03	0.25	0.18	0.08	0.01	0.10	0.00	0.09	0.03	0.08	0.03	0.09	0.01
K_2O	0.18	0.09	0.34	0.11	0.17	0.18	0.29	0.30	0.37	0.15	0.38	0.08	0.35	0.00	0.28	0.07	0.16	0.09
TiO_2	0.01	0.02	0.13	0.19	0.00	0.00	0.18	0.26	0.03	0.04	0.67	0.75	0.03	0.04	0.49	0.11	0.03	0.08
MnO	0.01	0.02	0.02	0.05	0.00	0.00	0.00	0.00	0.03	0.03	0.02	0.03	0.04	0.06	0.00	0.00	0.01	0.02
Total	98.70	0.67	99.63	0.60	99.97	0.50	99.22	0.31	95.67	0.73	94.74	0.65	94.96	0.28	95.81	0.44	95.27	0.46
	Structural formula, based on 8 atoms of oxygen																	
Si *apfu*	2.06	0.02	2.08	0.03	2.06	0.02	2.04	0.06	2.10	0.07	2.14	0.07	2.19	0.14	2.14	0.08	2.06	0.01
Al	1.87	0.02	1.85	0.02	1.87	0.02	1.90	0.04	1.84	0.08	1.77	0.08	1.78	0.14	1.77	0.09	1.88	0.02
Fe^{2+}	0.01	0.02	0.00	0.00	0.00	0.00	0.00	0.00	0.00	0.00	0.00	0.00	0.00	0.00	0.01	0.00	0.00	0.00
Ca	0.00	0.00	0.00	0.00	0.01	0.01	0.00	0.00	0.01	0.01	0.00	0.00	0.00	0.00	0.00	0.00	0.00	0.00
Ba	1.04	0.03	1.02	0.02	1.06	0.02	1.01	0.07	1.00	0.04	0.96	0.01	0.94	0.07	1.00	0.03	1.03	0.01
Na	0.02	0.01	0.03	0.01	0.02	0.00	0.03	0.02	0.01	0.00	0.01	0.00	0.01	0.00	0.01	0.00	0.01	0.00
K	0.01	0.01	0.03	0.01	0.01	0.01	0.03	0.02	0.03	0.01	0.03	0.01	0.03	0.00	0.02	0.01	0.01	0.01
Ti	0.00	0.00	0.01	0.01	0.00	0.00	0.01	0.01	0.00	0.00	0.03	0.04	0.00	0.00	0.02	0.00	0.00	0.00
% Cn	96.3	2.1	94.6	1.8	96.4	1.3	94.3	4.2	95.3	1.1	92.7	3.7	95.6	0.1	94.3	1.8	97.3	0.9
% Or	1.4	0.7	2.5	0.8	1.2	1.3	2.8	2.1	3.0	1.2	3.0	0.4	2.9	0.2	2.2	0.5	1.3	0.7
% Ab	2.1	1.3	2.7	0.8	1.8	0.4	2.8	2.1	1.0	0.2	1.2	0.1	1.2	0.3	1.0	0.4	1.1	0.2
% An	0.1	0.2	0.1	0.1	0.5	0.9	0.0	0.0	0.5	0.6	0.1	0.1	0.2	0.2	0.1	0.2	0.1	0.1

σ standard deviation, *n* number of samples, (*) total iron as FeO. The compositions were determined by electron-microprobe analysis.

TABLE 2. COMPOSITION OF HYALOPHANE AND K-FELDSPAR, SEDEX DEPOSITS, ZAMORA, SPAIN

	Hyalophane						K-feldspar							
Sample	IF-11	PB-3	PB-3	PB-3	PB-3	PB-3	SB-C	SB-C	SB-C	SB-C	SB-C	SB-C	SB-C	SB-C
Analysis	B3-3	1	2	3	4	5	2	3	5	6	7	8	9	10
SiO_2 wt%	51.07	50.35	51.63	49.86	54.53	52.43	63.26	64.13	62.69	62.91	64.62	64.22	63.68	64.18
Al_2O_3	20.81	20.74	20.98	20.59	19.66	20.11	17.90	17.48	17.86	18.35	17.79	17.71	18.08	18.09
FeO(*)	0.15	0.07	0.06	0.00	0.00	0.00	0.02	0.03	0.00	0.05	0.00	0.00	0.05	0.26
MgO	0.00	0.00	0.00	0.01	0.00	0.00	0.00	0.00	0.00	0.18	0.02	0.02	0.00	0.13
CaO	0.00	0.00	0.00	0.00	0.03	0.00	0.00	0.00	0.00	0.00	0.00	0.00	0.00	0.00
BaO	17.37	18.38	17.83	19.49	14.61	17.38	2.73	1.08	2.90	2.03	1.09	0.74	2.35	1.11
Na_2O	0.57	0.43	0.52	0.35	0.55	0.45	0.03	0.00	0.01	0.04	0.03	0.01	0.03	0.01
K_2O	8.78	8.35	8.53	8.61	10.02	9.71	16.20	17.17	15.96	15.84	16.63	16.73	16.25	16.12
TiO_2	0.00	0.99	0.80	0.00	0.02	0.00	0.01	0.00	0.01	0.00	0.02	0.03	0.01	0.04
MnO	0.05	0.09	0.14	0.04	0.00	0.00	0.00	0.00	0.00	0.04	0.01	0.00	0.00	0.00
Total	98.81	99.40	100.47	98.95	99.41	100.08	100.17	99.90	99.42	99.44	100.23	99.47	100.46	99.93
Structural formula, based on 8 atoms of oxygen														
Si *apfu*	2.69	2.65	2.67	2.66	2.79	2.73	2.98	3.01	2.98	2.97	3.01	3.01	2.98	2.99
Al	1.29	1.29	1.28	1.30	1.18	1.23	0.99	0.97	1.00	1.02	0.98	0.98	1.00	0.99
Fe	0.01	0.00	0.00	0.00	0.00	0.00	0.00	0.00	0.00	0.00	0.00	0.00	0.00	0.01
Mg	0.00	0.00	0.00	0.00	0.00	0.00	0.00	0.00	0.00	0.01	0.00	0.00	0.00	0.01
Ba	0.36	0.38	0.36	0.41	0.29	0.35	0.05	0.02	0.05	0.04	0.02	0.01	0.04	0.02
Na	0.06	0.04	0.05	0.04	0.05	0.05	0.00	0.00	0.00	0.00	0.00	0.00	0.00	0.00
K	0.59	0.56	0.56	0.59	0.65	0.64	0.97	1.03	0.97	0.95	0.99	1.00	0.97	0.96
Ti	0.00	0.04	0.03	0.00	0.00	0.00	0.00	0.00	0.00	0.00	0.00	0.00	0.00	0.00
% Cn	35.5	38.4	36.8	39.5	29.2	33.9	4.9	1.9	5.3	3.7	2.0	1.3	4.2	2.1
% Or	58.5	56.7	57.3	56.8	65.2	61.7	94.8	98.1	94.7	94.5	97.6	98.4	95.5	97.0
% Ab	5.7	4.5	5.3	3.5	5.4	4.4	0.3	0.0	0.0	0.4	0.3	0.1	0.3	0.0

(*) total iron as FeO. Structural formulae are expressed in *apfu*, atoms per formula unit. The compositions were obtained by electron-microprobe analysis.

as part of the quaternary feldspar system. They suggested that near the solidus of the series (high-T structural state), celsian is confined to 90–100 mole % Cn, whereas in the low-T structural state, corresponding to conditions prevalent at Aberfeldy, there is a composition gap between hyalophane (15–65 mole % Cn) and celsian (80–100 mole % Cn). The data presented here on celsian mostly fall above 90 mole % Cn, whereas hyalophane falls within the range 24–40 mole % Cn, consistent with the presence of a substantial compositional gap.

GENESIS

The petrographic relationships, in combination with the chemical data, provide evidence of the replacement of massive fine-grained barite by Ba-rich feldspars. The alternation of massive fine-grained thin layers of celsian with other thin layers of fine-grained barite, microcrystalline to cryptocrystalline apatite and sulfides (pyrite) is considered a primary sedimentary feature. Consequently the (Ba,K)-feldspars studied are considered to have formed *via* one of these processes: i) by replacement of authigenic barite, and ii) as an authigenic phase formed from an originally Ba–Al–Si gel. The merits of these hypotheses are now reviewed.

i) The replacement of authigenic barite occurred during a late diagenetic or metamorphic event. It was redissolved and reprecipitated as a result of a more reducing environment (Moro *et al.* 1994), and the barium was reprecipitated as Ba-rich feldspars. The presence of relict barite in some grains of celsian, hyalophane and cymrite (Figs. 3e, f) and the replacement of the barite (Figs. 4a, b) support the suggestion, as do the isotopic characteristics of the barite and associated sulfides and carbonates (Moro *et al.* 1994). During metamorphic processes, and mainly during the early stage of diagenesis, barite dissolution could have occurred in an environment where the Eh value may have reached < –300 mV, with neutral or slightly alkaline pH values. Such a process of dissolution could have been aided by the presence of bacteria able to reduce the sulfates and metabolize the ^{32}S and ^{16}O (Mizutani & Rafter 1973, McCready & Krouse 1980). The barite that reprecipitated later, in more oxidizing environments, would be enriched in ^{34}S and ^{18}O. Major products of this reduction process are CO_2 and H_2S, which can form the associated carbonates and sulfides.

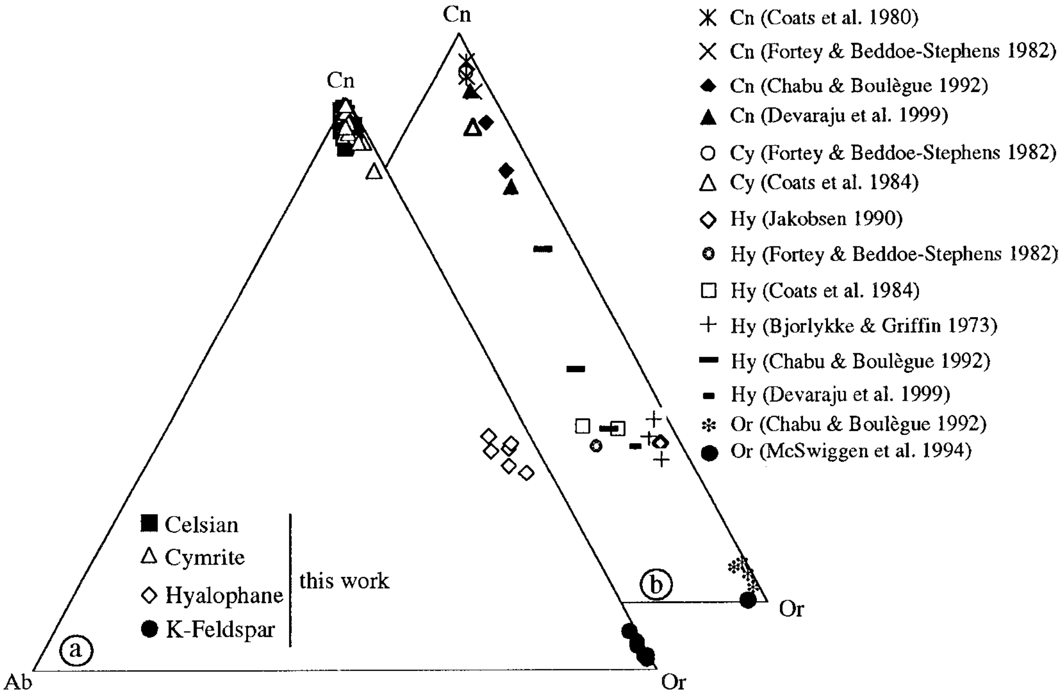

FIG. 5. Composition of the (Ba, K)-feldspars: (a) in the samples studied and (b) from the literature, in terms of albite (Ab), orthoclase (Or) and celsian (Cn).

ii) It is possible that massive fine-grained beds of celsian and barite, phosphate and sulfides already constituted penecontemporaneous chemical precipitates (authigenic phases). According to Coats *et al.* (1980), the textural relationships among them suggest that these beds of Ba-rich feldspar formed from what was originally a Ba–Al–Si gel. In this model, the process by which the (Ba,K)-feldspars were formed was multistaged, beginning with harmotome ($BaAl_2Si_6O_6•6H_2O$) or an unnamed hydrous Ba-silicate ($BaAl_2Si_2O_8•4H_2O$) (Jakobsen 1990). Following a series of essentially dehydration-type reactions, these phases reacted to form cymrite ($BaAl_2Si_2O_8•nH_2O$), and finally celsian ($BaAl_2Si_2O_8$) (Jakobsen 1990, Matsubara 1985, Fortey & Beddoe-Stephens 1982). Ba, SiO_2, and P were supplied to the basin by hydrothermal activity (Moro *et al.* 1994). Barium and silica was most probably kept as a silica gel on the sea floor (Large 1980) and during later diagenesis, under relatively reducing and calcareous conditions, barite, Ba-silicates and phosphate formed simultaneously.

Textural evidence indicates that the cymrite could represent an intermediate phase in a prograde diagenetic sequence of minerals, for example at the expense of harmotome ($BaAl_2Si_6O_6•6H_2O$) through a stage of hydrated Ba silicate ($BaAl_2Si_2O_8•4H_2O$) (Jakobsen 1990), to cymrite, and ending with celsian with increasing P–T conditions. Assuming rapid reaction between cymrite and celsian, as observed by Nitsch (1980) in his hydrothermal experiments, all the cymrite should have reacted to celsian + H_2O. Later, this celsian was partially hydrated again to form cymrite, as indicated by the textural relationships describe above. The relics of celsian observed may have escaped the reaction because locally $P(H_2O)$ may have been lower than P_{fluid}. From textural evidence, cymrite grew at a late stage by replacement of celsian and also, in some cases, by replacement of a pre-existing mineral, most likely barite.

Moro *et al.* (1994) deduced a temperature of 350°–370°C and a pressure of 1.5 kbars from fluid inclusions, and the presence of vitrinite at approximately 350°C would indicate the upper limit of P–T reached by these zones of mineralization. These values are consistent with those reported by González Clavijo (1997) from the *b* parameter of the illite hosting the barite deposits, and particularly with those reported by Barrenechea *et al.* (1992) from the ^{IV}Al content of chlorite and the C_0 parameter of graphite in similar Silurian sedimentary rocks.

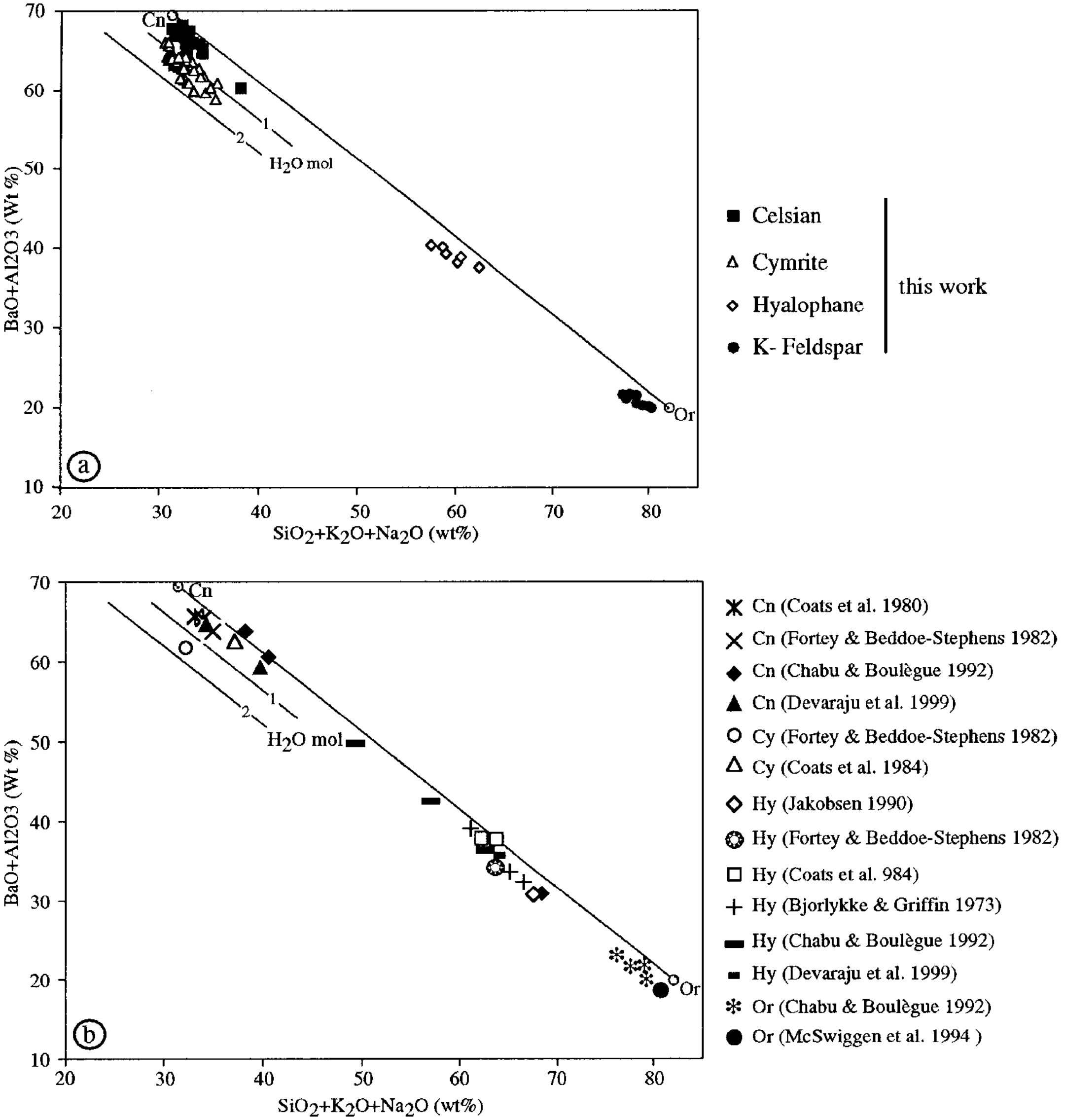

FIG. 6. BaO + Al_2O_3 *versus* SiO_2 + K_2O + Na_2O (wt%) for celsian (Cn), cymrite (Cy) and hyalophane (Hy): (a) from the (Ba,K)-feldspars studied and (b) from the literature.

Consequently, the upper limit of P–T reached by these mineralized rocks during regional metamorphic processes was near the reaction curve celsian + H_2O = cymrite (Essene 1967). On the basis of the equilibrium location of this reaction, investigated by Seki & Kennedy (1964), Nitsch (1980) and Graham *et al.* (1992), cymrite is only stable at high pressures. The numerous documented occurrences of cymrite in low-P – low-T sedimentary and hydrothermal environments are considered to be the result of its metastable growth and persistence in the stability field of celsian. Hsu (1994) proved that cymrite found in Nevada in a low-grade metamorphosed Cambrian sequence of barite beds, can be stable at much lower pressures than those previously reported. The apparent stability of cymrite in the Paleozoic sedex barite deposits of Zamora at 350°–370°C and 1.5 kbars confirms that this mineral can be stable in low P–T metasedimentary environments.

ACKNOWLEDGEMENTS

This work was supported by the Comunidad Autónoma de Castilla y León (Research Project SA 54 /97) and by the I+D Project, FEDER Program (Ref. 1FD97–0235). We thank Dr. Frank W. Dickson and an anonymous referee, as well as Robert F. Martin for their helpful comments.

REFERENCES

AYE, F.& STRAUSS, G.K. (1975): Identification de cymerite (Ba,Al,Si_3O_8OH) dans la province sud-ibérique: minéraux associés (La Zarra, Huelva, Espagne). *C.R. Acad. Sci. Paris* **D281**, 1935-1938.

BARRENECHEA, J.F., RODAS, M. & ARCHE, A. (1992): Relation between graphitization of organic matter and clay mineralogy: Silurian black shales in central Spain. *Mineral. Mag.* **56**, 477-485.

BJORLYKKE, K.O. & GRIFFIN, W.L. (1973): Barium feldspars in Ordovician sediments, Oslo region, Norway. *J. Sed. Petrol.* **43**, 461-465.

CARRON, M.K., MROSE, M.E. & REISER, H.N. (1964): New data on cymrite, a hydrated silicate of barium and aluminium. *Geol. Soc. Am., Spec. Pap.* **82**, 26 (abstr.).

CHABU, M. & BOULÈGUE, J. (1992): Barian feldspar and muscovite from the Kipushi Zn–Pb–Cu deposit, Shaba, Zaire. *Can. Mineral.* **30**, 1143-1152.

COATS, J.S., FORTEY, N.J., GALLAGHER, M.J. & GROUT, A. (1984): Stratiform barium enrichment in the Dalradian of Scotland. *Econ. Geol.* **79**, 1585-1595.

________, SMITH, C.G., FORTEY, N.J., GALLAGHER, M.J., MAY, F. & MCCOURT, W.J. (1980): Strata-bound barium-zinc mineralization in Dalradian schist near Aberfeldy, Scotland. *Trans. Inst. Mining Metall., Sect. B: Appl. Earth Sci.* **89**, 110-122.

CLAYPOOL, G.E., HOLSER, W.T., KAPLAN, I.R., SAKAI, H. & ZAK, I. (1980): The age curves of sulfur and oxygen isotopes in marine sulfate and their mutual interpretation. *Chem. Geol.* **28**, 199-260.

DEER, W.A., HOWIE, R.A. & ZUSSMAN, J. (1992): *An Introduction to the Rock-Forming Minerals* (second ed.). Longman, London, U.K.

DEVARAJU, T.C., RAITH, M.M. & SPIERING, B. (1999): Mineralogy of the Archean barite deposit of Ghattihosahalli, Karnataka, India. *Can. Mineral.* **37**, 603-617.

ESSENE, E.J. (1967): An occurrence of cymrite in the Franciscan Formation, California. *Am. Mineral.* **52**, 1885-1890.

FORTEY, N.J. & BEDDOE-STEPHENS, B.(1982): Barium silicates in stratabound Ba–Zn mineralization in the Scottish Dalradian. *Mineral. Mag.* **46**, 63-72.

________, COATS, J.S., GALLAGHER, M.J., SMITH, C.G. & GREENWOOD, P.G. (1993): New strata-bound barite and base metals in Middle Dalradian rocks near Braemar, northeast Scotland. *Trans. Inst. Mining Metall., Sect. B, Appl. Earth Sci.* **102**, 55-64.

FROEHLICH, F. & SANDRÉA, A. (1973): Présence de cymrite dans les minéralisations dévoniennes stratiformes à blende – galène – barytine d'Arrens (Haute-Pyrénées). *C.R. Acad. Sci. Paris.* **D277**, 2445-2448.

GAY, P. & ROY, N.N. (1968): The mineralogy of the potassium–barium feldspar series. III. Subsolidus relationships. *Mineral. Mag.* **36**, 914-932.

GONZÁLEZ CLAVIJO, E. (1997): *La geología del Sinforme de Alcañices, oeste de Zamora.* Ph.D. thesis, Univ. de Salamanca, Salamanca, Spain.

GRAHAM, C.M., TAREEN, J.A.K., MCMILLAN, P.F. & LOWE, B.M. (1992): An experimental and thermodynamic study of cymrite and celsian stability in the system BaO–Al_2O_3–SiO_2–H_2O. *Eur. J. Mineral.* **4**, 251-269.

HERNÁNDEZ, E., MORO, M.C. & CEMBRANOS, M.L. (1991): Contribution of the study of fluid inclusions to the genesis of Paleozoic stratiform barites in the province of Zamora (Spain). *Plinius* **5**, 102-103.

HSU, L.C. (1994): Cymrite: new occurrence and stability. *Contrib. Mineral. Petrol.* **118**, 314-320.

JAKOBSEN, U.H. (1990): A hydrated barium silicate in unmetamorphosed sedimentary rocks of central North Greenland. *Mineral. Mag.* **54**, 81-89.

KRÌBEK, B., HLADÍKOVÁ, J., ZÁK, K., BENDL, J., PUDILOVÁ, M. & UHLÍK, Z. (1996): Barite–hyalophane sulfidic ores at Rozna, Bohemian Massif, Czech Republic: metamorphosed black shale-hosted submarine exhalative mineralization. *Econ. Geol.* **91**, 14-35.

LARGE, D.E. (1980): Geological parameters associated with sediment-hosted, submarine exhalative Pb–Zn deposits: an empirical model for mineral exploration: *Geol. Jahrb.* **40**, 59-129.

LIN, H.C. & FOSTER, W.R. (1968): Studies in the system BaO–Al_2O_3–SiO_2. I. The polymorphism of celsian. *Am. Mineral.* **53**, 134-144.

MATSUBARA, S. (1985): The mineralogical implication of barium and strontium silicates. *Bull. Nat. Sci. Mus. Tokyo, Ser.* **C 11**(2), 1-95.

MCCREADY, R.D.L. & KROUSE, H.R. (1980): Sulfur isotope fractionation by *Desulfovibrio vulgaria* during metabolism of $BaSO_4$. *Geomicrobiol. J.* **2**, 55-62.

MCSWIGGEN, P.L., MOREY, G.B. & CLELAND, J.M. (1994): Occurrence and genetic implications of hyalophane in manganese-rich iron-formation, Cuyuna Iron Range, Minnesota, USA. *Mineral. Mag.* **58**, 387-399.

MIZUTANI, Y. & RAFTER, T.A. (1973): Isotopic behavior of sulphate oxygen in the bacterial reduction of sulphate. *Geochem. J.* **6**, 183-191.

MOLES, N.R. (1985): Metamorphic conditions and uplift hystory in central Perthshire: evidence from mineral equilibria in the Foss celsian – barite – sulphide deposit, Aberfeldy. *J. Geol. Soc. London* **142**, 39-52.

MORO, M.C., PÉREZ DEL VILLAR, L. & CEMBRANOS, M.L. (1993): Cymrite in the stratiform barite deposits of Zamora Province (central W Spain). *In* Current Research in Geology Applied to Ore Deposits (P. Fenoll, J. Torres Ruiz & F. Gervilla, eds.). Univ. Granada, Granada, Spain (175-178).

________, ________ & ________ (1994): Stratiform barite ore deposits in Palaeozoic rocks, Province of Zamora (Spain). *In* Metallogeny of Collisional Orogens (R. Seltmann, H. Kämpf & P. Möller, eds.). Czech Geological Survey, Prague, Czech Republic (376-382).

NITSCH, K.H. (1980): Reaktion von Barium Feldspat (Celsian) mit H_2O zu Cymrit unter metamorphen Bedingungen. *Fortschr. Mineral*. **58**, 98-100.

PAN, YUANMING & FLEET, M.E. (1991): Barian feldspar and barian-chromian muscovite from the Hemlo area, Ontario. *Can. Mineral*. **29**, 481-498.

POOLE, B., MORO, M.C., LOPERA, E. & ARRIBAS, A. (1990): Setting and origin of stratiform barite and associated rocks of the Hercynian orogen in western Spain. *Int. Assoc. on the Genesis of Ore Deposits, Program Abstr., 8th Symp.* (*Ottawa*), A21-A22.

POUIT, G. & BOIS, J.P. (1986): Arrens Zn(Pb), Ba Devonian deposits, Pyrénées, France: an exhalative-sedimentary type deposit similar to Meggen. *Mineral. Deposita* **21**, 181-189.

QUIROGA, J.L. (1981): *Estudio geológico del Paleozoico del W de Zamora* (*Alba y Aliste*). Ph.D. thesis, Univ. de Oviedo, Oviedo, Spain.

REINECKE, T. (1982): Cymrite and celsian in manganese-rich metamorphic rocks from Andros Island/Greece. *Contrib. Mineral. Petrol.* **79**, 333-336.

RUNNELLS, D.D. (1964): Cymrite in a copper deposit, Brooks Range, Alaska. *Am. Mineral.* **49**, 158-165.

SEKI, Y. & KENNEDY, G.C. (1964): Phase relations between cymrite, $BaAlSi_3O_8(OH)$ and celsian, $BaAl_2Si_2O_8$. *Am. Mineral*. **49**, 1407-1426.

SOONG, R. & OLIVECRONA, J.A.C. (1975): An occurrence of cymrite in black shale, north-west Nelson, South Island, New Zealand. *Mineral. Mag*. **40**, 311-312.

VISWANATHAN, K., HARNEIT, O. & EPPLE, M. (1992): Hydrated barium aluminosilicates, $BaAl_2Si_2O_8 \bullet nH_2O$, and their relations to cymrite and hexacelsian. *Eur. J. Mineral.* **4**, 271-278.

Received February 29, 2000, revised manuscript accepted July 4, 2001.